Wind Forecasting Using Kriging and Vector Auto-Regressive Models for Dynamic Line Rating Studies

Fulin Fan, Keith Bell, David Hill and David Infield
Department of Electronic and Electrical Engineering
University of Strathclyde
Glasgow, United Kingdom
f.fan@strath.ac.uk

***Abstract*—This paper aims to describe methods to forecast wind speeds experienced around overhead lines (OHLs) in order to predict the wind cooling effect and thus the dynamic line ratings (DLRs) of OHLs. The wind speed at a particular OHL span is forecast through a kriging interpolation between the wind speed predictions produced by a vector auto-regressive (VAR) model for a limited number of weather stations at which observations have been obtained. A temporal de-trending method is used to ensure the stationarity of de-trended data from which model parameters are determined. A spatial de-trending method is adopted in a kriging model. The results show that the kriging model performs better than the inverse distance weighting (IDW) method and that the spatial de-trending makes the main contribution to the accuracy of interpolation. Furthermore, the VAR forecasting model is shown to give greater improvement over persistence than a simple auto-regressive (AR) model.**

***Index Terms*-- Dynamic line rating, Kriging, Vector auto-regressive models, De-trending**

I. INTRODUCTION

The dynamic thermal rating (DTR) or real-time thermal rating (RTTR) is the highest current at which a branch of a transmission or distribution network can be operated at safely and reliably at the time in question [1]. In the case of overhead lines (OHLs), RTTR is typically referred to as dynamic line rating (DLR) [2]. A DLR system can estimate or predict the line ampacity and offer evidence to network operators of the safe levels of power flow on network branches. A number of techniques have been developed to quantify the DLRs of OHLs through direct measurement or inference of the span sag or conductor temperature [3]-[7]. In investment planning timescales, DLRs can be considered over a range of future operating conditions and offer a cost-effective means to deal with power generation and demand growth or distributed generation connections that reduce the need for network reinforcements.

A weather model for DLR estimation using real-time meteorological data combined with a thermal model of overhead conductors [8]-[10] and an inverse distance weighting (IDW) interpolation method to infer weather conditions for each span of the OHL was successfully developed by Durham University [1], [11]. Building on Durham's work, an enhanced weather model is being developed with the ability to not only provide real-time ratings but also forecasts of ratings so that system or wind farm operators have time to take action to mitigate the consequences of the limitations of power transfer or, alternatively and where possible, to exploit additional thermal capacity. Moreover, an informed judgment about risk may be made in advance if the DLR forecast is lower than the static ratings.

IDW interpolation using a wind profile power law was applied in Durham's work [11]. Spatial interpolation methods for wind speed including IDW, kriging and co-kriging, etc. were compared in [12]; co-kriging performed best due to the inclusion of elevations of the weather stations. As a substitute for co-kriging, a kriging model combined with a surface or spatial de-trending (SD) in terms of distance to ocean (DTO) and elevation is developed in this paper.

An advanced spatio-temporal model making use of the vector auto-regressive (VAR) model and temporal de-trending to extract annual and seasonally varying diurnal trends [13] is adopted to forecast wind speeds at a limited number of weather stations at which historic observations are obtained.

The 10-minute average wind speed data are provided by Scottish Power Energy Networks (SPEN) from their project of "Implementation of real-time thermal ratings" (LNCF SPT1001) in North Wales [14]. A map of the research area is shown in Fig. 1.

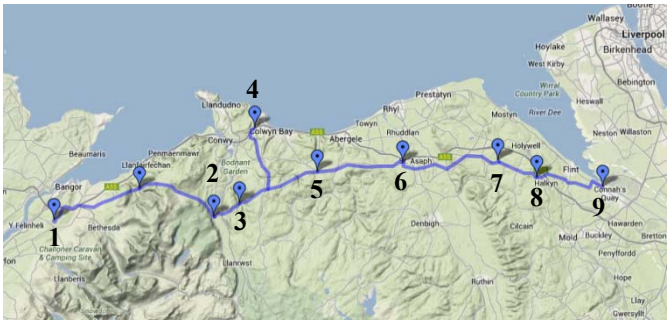

Fig. 1. Map showing locations of 9 weather stations in North Wales.

This project is funded by the Scottish 'Energy Technology Partnership (ETP)', the University of Strathclyde, Scottish Power Energy Networks (SPEN) and National Grid Electricity Transmission (NGET).

II. METHODOLOGY

A. Temporal De-Trending

Data applied to statistical models, like kriging and vector auto-regressive (VAR) models, are generally required to satisfy a weak or second order stationarity. That is, neither the mean nor the variance of the data should vary with time and the auto-covariance is dependent on the time lag only [15]. The inherent trends of non-stationary data may be misleading with regard to correlations among variables or the auto-correlation of a time series. Therefore, any trend implied in the non-stationary data should be removed before the applications of the kriging and VAR models.

The annual trend and seasonally varying diurnal trends of wind speed data at each weather station are separately modelled by a Fourier series of a reasonable order of p [16]:

$$Trend = F_0 + \sum_{i=1}^{p} F_i \sin(iwt + \varphi_i) \qquad (1)$$

where terms F_i and φ_i are the Fourier coefficients of the i^{th} harmonics. The term F_0 is the offset of data and w represents the frequency. The hourly wind speeds in the year 2006-2007 measured at the British Atmospheric Data Centre (BADC) weather station Rhyl located in North Wales are used to illustrate the process of temporal de-trending.

The annual trend is first well modelled by a Fourier series of order equal to six with the annual angular frequency of $2\pi/(365 \times 24)$, as shown in Fig. 2. Then, the fitted annual trend is subtracted from the original data of wind speed.

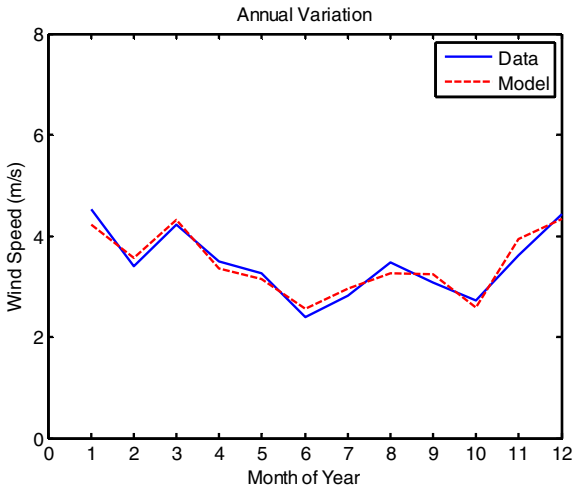

Fig. 2. Modelling of annual trend at Rhyl.

Previous work has found that the diurnal trend, especially at coastal locations, varies through the year [13]. As a consequence, the data without the annual trend are categorized into four groups according to four seasons, spring (March to May), summer (June to August), autumn (September to November) and winter (December to February). The diurnal trend in each season is then fitted to the data in the corresponding bin by a Fourier series of order equal to four with the diurnal angular frequency of $2\pi/24$ [13] as shown in Fig. 3. The diurnal trends in spring and summer are similar and more obvious than those in autumn and winter.

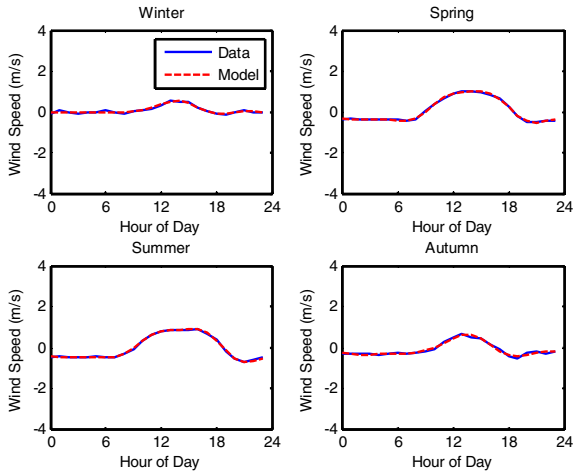

Fig. 3. Modelling of diurnal trends in four seasons at Rhyl.

Finally, the modelled diurnal trends in different seasons and the annual trend are all removed from the original data so as to obtain the de-trended data with a reasonable degree of stationarity. These de-trended data will be applied to determine the parameters of the kriging and VAR models.

B. Inverse Distance Weighting and Kriging

Inverse distance weighting (IDW) and kriging both infer the wind speed at a target location as a weighted sum of observations at surrounding sampled locations [17]:

$$y(u_o) - m(u_o) = \sum_{i=1}^{n(u)} \lambda_i [y(u_i) - m(u_i)] \qquad (2)$$

where $y(u_o)$ and $y(u_i)$ are values at the target location u_o and sampled location u_i respectively. The terms $m(u_o)$ and $m(u_i)$ are the expected values or trend components of $y(u_o)$ and $y(u_i)$. $n(u)$ is the number of sampled locations and λ_i is the weight assigned to the sampled location u_i.

The IDW weights $\lambda_{IDW,i}$ are inversely proportional to the distances $d_{i,o}$ between u_o and u_i:

$$\lambda_{IDW,i} = \frac{1/d_{i,o}^{q}}{\sum_{i=1}^{n(u)} \left(1/d_{i,o}^{q}\right)} \qquad (3)$$

where q is a power parameter equal to 2 in [11].

The kriging weights $\lambda_{KRI,i}$ are determined to minimize the variance of estimation errors. In addition to the distance $d_{i,o}$, kriging weights depend largely on the spatial relationships between variables at all locations [17]:

$$\lambda_{KRI,i} = \boldsymbol{K}^{-1}\boldsymbol{k} \qquad (4)$$

where $\boldsymbol{K}$ represents the matrix of covariances between the sampled locations and $\boldsymbol{k}$ is the vector of covariances between the target and sampled locations.

The elements in both $\boldsymbol{K}$ and $\boldsymbol{k}$ are estimated as a function in terms of distance which is fitted to the empirical semi-variances $\gamma(h)$ [18]:

$$\gamma(h) = \frac{1}{2n(h)} \sum_{i=1}^{n(h)} [y(x_i) - y(x_i + h)]^2 \quad (5)$$

where $n(h)$ is the number of pairs of observations $y(x_i)$ and $y(x_i + h)$ which are a distance lag h apart. The semi-variance generally increases with the distance within a range. In our work a spherical model [18] is used to fit the empirical semi-variances:

$$\gamma^*(h) = \begin{cases} 0 & h = 0 \\ b + c\left[1.5\left(\frac{h}{a}\right) - 0.5\left(\frac{h}{a}\right)^3\right] & 0 < h \le a \\ b + c & h > a \end{cases} \quad (6)$$

where the coefficient b is named as the "nugget" representing the spatially uncorrelated noises. The coefficient a is the "range" at which the semi-variance just reaches the maximum value $(b + c)$ known as the "sill" [18]. These coefficients are determined by the least squares fitting and the elements of covariance $C(h)$ in $\boldsymbol{K}$ and $\boldsymbol{k}$ can be estimated via the equation:

$$C(h) = Sill - \gamma^*(h) \quad (7)$$

The calculated covariance between two locations separated by a distance in excess of the "range" is zero, implying that they have no impact on each other.

C. Spatial De-Trending

Spatial de-trending (SD) is used to remove trend surfaces which are fitted to weather data in terms of the geographic variables of interest. These trend surfaces are then added back in the interpolations at the end of the IDW or kriging process. In this manner, the effects of these geographic variables on the spatial correlations can be mitigated [19].

Before modelling the trend surfaces, the wind speeds v_{ane} at the anemometers' heights z_{ane} are converted to a common reference level z_{ref} taking the ground roughness lengths z_o into account through the equation [20]:

$$v_{ref} = v_{ane} \frac{\ln(z_{ref}/z_o)}{\ln(z_{ane}/z_o)} \quad (8)$$

The IDW and kriging interpolations, as well as the subtraction and addition of trend surfaces are all done at the reference level. The interpolation results at the reference level are then converted back to the elevation of the target location.

A reference height of 200m above ground level (AGL) is adopted in Durham's work and 300m above sea level (ASL) is chosen in this paper as a comparison. In order to minimize the spatial variation further, the trend surfaces of wind speeds v_{ref} at the reference level (300m ASL) are modelled in terms of DTO and elevation as shown in Fig. 4. The weather stations at higher elevations and closer to the coast are generally shown to have higher wind speed averages in this case, which is also discovered by Nawri [21] and Xue [22].

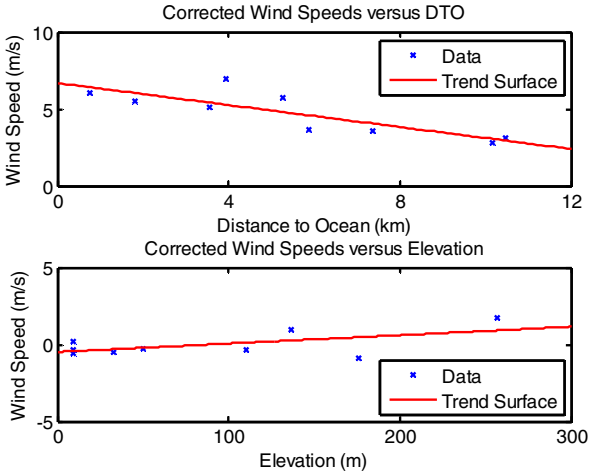

Fig. 4. The trend surface of corrected wind speeds at 300m ASL in terms of distance to ocean (DTO) and that in terms of elevation after removing the trend surface modelled in terms of DTO.

D. Auto-Regressive and Vector Auto-Regressive Models

The auto-regressive (AR) model of order p estimates the forecast $\tilde{z}_t$ as a linear combination of p historical values at a target location and a random shock e_t [23]:

$$\tilde{z}_t = \sum_{i=1}^{p} \emptyset_i \tilde{z}_{t-i} + e_t \quad (9)$$

where $\tilde{z}_t$ represents the deviation from the expected value or trend component and $\emptyset_i$ is the auto-regressive parameter.

As an extension of a univariate AR model, the vector auto-regressive (VAR) model of order p offers a way of producing the forecast as a weighted sum of historical time series not only at the target location but also from its surrounding sampled locations [24]:

$$\tilde{\boldsymbol{Z}}_t = \boldsymbol{u} + \sum_{i=1}^{p} \boldsymbol{A}_i \tilde{\boldsymbol{Z}}_{t-i} + \boldsymbol{E}_t \quad (10)$$

where $\tilde{\boldsymbol{Z}}_t$ is a $(K \times 1)$ vector consisting of $\tilde{z}_t$ at K locations and $\boldsymbol{u}$ is a $(K \times 1)$ vector of the non-zero means of $\tilde{\boldsymbol{Z}}_t$. $\boldsymbol{A}_i$ represents a $(K \times K)$ matrix of coefficients at time lag i and $\boldsymbol{E}_t$ is a $(K \times 1)$ vector of innovation process.

$$\tilde{\boldsymbol{Z}}_t = \begin{bmatrix} \tilde{z}_{1t} \\ \tilde{z}_{2t} \\ \vdots \\ \tilde{z}_{Kt} \end{bmatrix} \quad \boldsymbol{u} = \begin{bmatrix} u_1 \\ u_2 \\ \vdots \\ u_K \end{bmatrix} \quad \boldsymbol{A}_i = \begin{bmatrix} A_{11}^i & \cdots & A_{1K}^i \\ \vdots & \ddots & \vdots \\ A_{K1}^i & \cdots & A_{KK}^i \end{bmatrix} \quad \boldsymbol{E}_t = \begin{bmatrix} e_{1t} \\ e_{2t} \\ \vdots \\ e_{Kt} \end{bmatrix}$$

The parameters in the AR or VAR model are estimated by using least squares fitting which is accomplished using MATLAB [25].

III. Results and Discussion

The accuracies of spatial interpolation methods are assessed by calculating and comparing their mean absolute (MA) errors and root mean squared (RMS) errors [26] when taking each weather station as the target location in a cross-validation procedure. The MA errors and RMS errors of the forecasting models over a look-ahead period of 2 hours at the 9 weather stations are compared with the errors of a persistence forecasting method which supposes that wind speeds in the future are equal to the present values [27].

A. *Inverse Distance Weighting and Kriging*

Four spatial interpolation methods are applied to the wind speed estimations:

- IDW, with a reference level at 200m AGL, without surface de-trending (IDW, 2AGL, w/o SD) which was used in the Durham's work;
- IDW, with a reference level at 300m ASL, without SD (IDW, 3ASL, w/o SD);
- IDW, with a reference level at 300m ASL, with SD (IDW, 3ASL, w SD);
- Kriging, with a reference level at 300m ASL, with SD (KRI, 3ASL, w SD).

The improvements in MA errors and RMS errors for wind speed interpolations over the Durham's method for the other three methods are shown in Fig. 5 and Fig. 6 respectively.

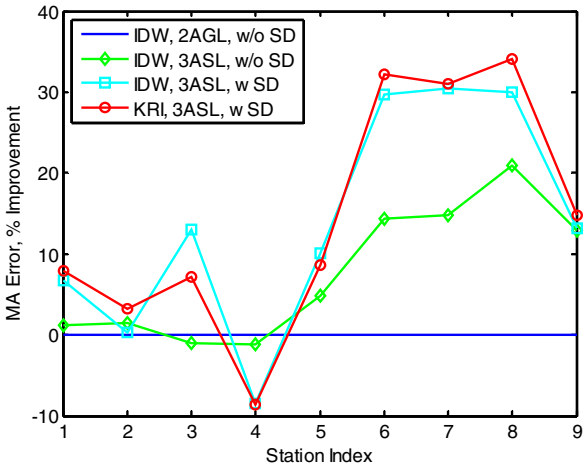

Fig. 5. Improvement in MA errors over Durham's method for other ones

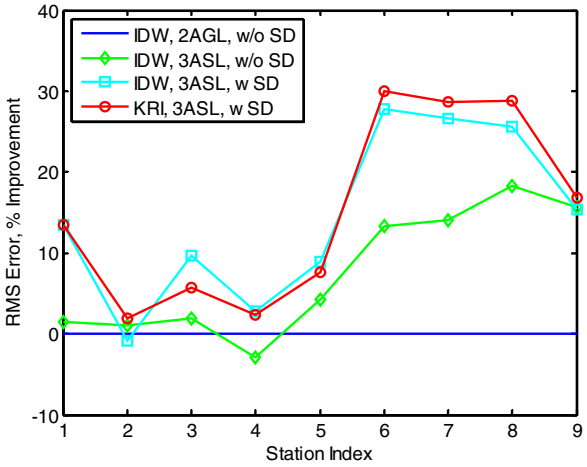

Fig. 6. Improvement in RMS errors over Durham's method for other ones

Both figures show that 300m ASL is a better choice as the reference level in this case where weather stations are located in the mountainous terrain, especially the stations 6-9.

Using the same reference level of 300m ASL and the IDW method, the additional application of spatial de-trending (SD) improves the accuracy of wind speed interpolation further. An exception is the improvement in MA error for weather station 4. As can be seen from Fig. 1, station 4 is the one closest to the coast and off the main OHL route so that the value of the trend surface in terms of DTO at station 4 is extrapolated and overestimated when station 4 is the target location. Fortunately, the values of the trend surfaces at locations of overhead conductors are all interpolated. Therefore, the underestimation or overestimation caused by the extrapolation of trend surfaces will not happen when estimating wind speeds at the OHL spans.

In addition, the kriging method performs just slightly better than the IDW method at most stations when both contain the SD. The limited improvement might be caused by the insufficient number and the distribution of weather stations. The limited number of stations results in the number of empirical semi-variance points not being enough to fit an accurate spherical model. That being said, the spatial correlation extracted from the finite empirical semi-variances is not reliable for a limited number of sampled locations.

Besides the distances from the target location, kriging weights are dependent on the spatial correlations not only between the sampled and target locations but also between the sampled locations themselves. In an isotropic region, i.e. one that has the same characteristics in all directions, the sum of kriging weights assigned to the sampled locations within a cluster is generally similar to the weight assigned to an isolated sampled location if they have the same distances from the target location [17]. Therefore, the effect of clusters can be mitigated by the kriging process. However, the weather stations in the research area are fairly well distributed and there are no severe clusters so that kriging's advantage of compensation for cluster effects is constrained.

B. *Auto-Regressive and Vector Auto-Regressive Models*

The parameters in the AR and VAR models are estimated based on the residuals after removing the temporal trends at each station. The wind speed prediction is constructed as a sum of the residual forecast and the corresponding fitted temporal trend at a given future moment.

The orders of the AR and VAR models can be confirmed through the inspection of partial autocorrelation functions [23] or the comparison of forecast errors for different model orders. The RMS errors of one-step-ahead forecasts at the station 6 (St. Asaph) produced by the AR and VAR models of different orders p as listed in Table I demonstrate that less than 0.5% improvements are achieved when orders are over 3. Therefore, wind speeds are forecast using the AR(3) and VAR(3) models.

TABLE I. RMS ERRORS OF AR AND VAR OF DIFFERENT ORDERS

	$p = 1$	$p = 2$	$p = 3$	$p = 4$	$p = 5$
AR	0.4354	0.4195	0.4157	0.4140	0.4133
VAR	0.4220	0.4112	0.4084	0.4070	0.4062

The improvements over persistence in MA errors and RMS errors of total wind speed forecasts for up to 2 hours ahead for the AR(3) and VAR(3) models are shown in Fig. 7 and Fig. 8.

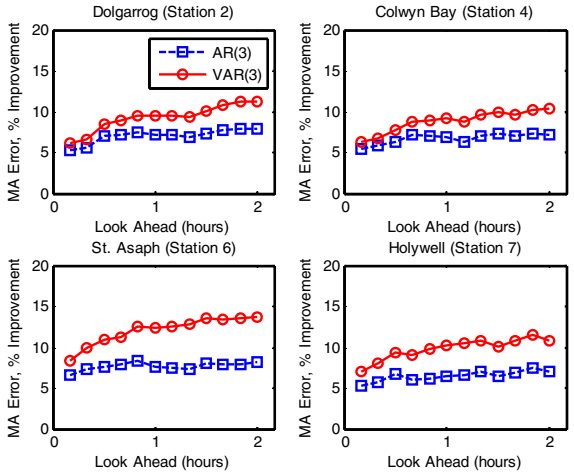

Fig. 7. Improvement over persistence in MA errors for up to 2h ahead for AR(3) and VAR(3) forecasting models at four stations.

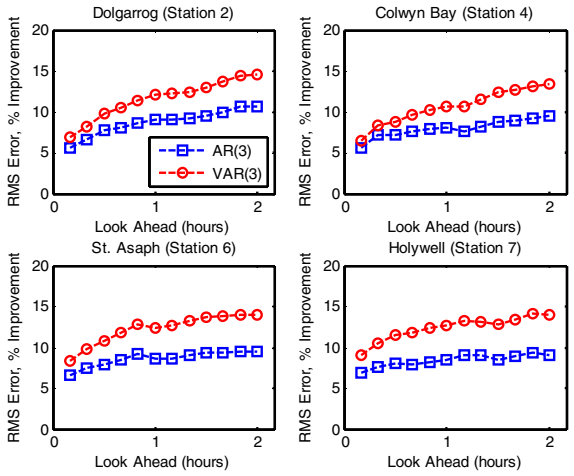

Fig. 8. Improvement over persistence in RMS errors for up to 2h ahead for AR(3) and VAR(3) forecasting models at four stations.

The VAR(3) forecasting model is shown to produce predictions with higher quality than the AR(3) model due to the additional capture of the inherent spatial correlations among the field data. In addition, the AR(3) or VAR(3) model usually has a more distinct improvement over persistence with the forecast horizon going further. Therefore, a VAR(3) forecasting model with the temporal de-trending is the better choice to forecast the wind speed in this case.

IV. Conclusion and Future Work

This paper has described and assessed different spatial interpolation methods and forecasting models in preparation for the future work of predicting the wind speeds at a set of OHL spans.

The kriging method with spatial de-trending and a reference level of 300m above sea level is a preferable approach for the wind speed interpolation compared with a reference level of 200m above ground and inverse distance weighting (IDW) used in previous work at Durham University. Using the new reference level and modelling trend surfaces makes the main contribution to the improvements in the qualities of interpolations. Kriging as an advanced interpolation method takes both the spatial correlations and distances between locations into consideration. However, only a slight enhancement in accuracy for kriging over the IDW method is obtained in this study. This seems to be due to the limited number of weather stations and their uniform distribution. It should be noted that it cannot be guaranteed that any particular spatial interpolation method will be suitable for all cases [28]. For different meteorological variables or study regions of interest, an appropriate spatial interpolation method in each case has to be obtained through many attempts of possible approaches.

Temporal de-trending provides a way to generate the de-trended data which satisfy a reasonable order of stationarity. VAR parameters calculated based on the wind speed residuals at each location could describe the spatio-temporal correlations between weather stations more reliably than a univariate AR model. Experiment results reveal that the VAR(3) forecasting model was preferred in this case.

Future work will continue to establish the optimum models for forecasting meteorological data of air temperature, wind direction and solar radiation which also have an impact on the thermal behavior of an overhead conductor. Then, these forecasting models will be developed further to provide prediction percentiles describing the probability of particular OHL thermal ratings being exceeded.

Acknowledgment

The authors gratefully acknowledge the supply of the meteorological data and the technical parameters from Scottish Power Energy Networks and the British Atmospheric Data Centre.

References

[1] A. Michiorri, P.C. Taylor, S.C.E. Jupe, and C.J. Berry, "Investigation into the influence of environmental conditions on power system ratings," *Proc. of the Institution of Mechanical Engineers, Part A: Journal of Power and Energy*, vol. 223, no. 7, pp. 743-757, Nov. 2009.

[2] D.J. Morrow, J. Fu, and S.M. Abdelkader, "Experimentally validated partial least squares model for dynamic line rating," *IET Renewable Power Generation*, vol. 8, issue 3, pp. 260-268, Apr. 2014.

[3] M. Gabrovsek and V. Lovrencic, "Temperature monitoring of overhead lines is Smart Grid solution for power grid," *Smart Grid 2010 Retele Energetic Intelligent Conf.*, Sibiu, Sep. 2010 [Online]. Available: http://www.otlm.eu/files/8268B60HIQV2GH8Q941585N2FBPIWLS7.pdf

[4] E. Golinelli, S. Musazzi, U. Perini, and F. Barberis, "Conductors sag monitoring by means of a laser based scanning measuring system: experimental results," *2012 IEEE Sensors Applications Symposium (SAS)*, pp. 1-4. Feb. 2012.

[5] Z. He and Y. Liu, "The field application analysis of dynamic line rating system based on tension monitoring," *2011 IEEE Power Engineering and Automation (PEAM) Conf.*, vol. 2, pp. 284-288, Sep. 2011.

[6] E. Cloet and J.L. Lilien, "Uprating transmission lines through the use of an innovative real-time monitoring system," *IEEE PES 12th Int. Conf. on Transmission and Distribution Construction, Operation and Live-Line Maintenance (ESMO)*, pp. 1-6, May 2011.

[7] J. Ausen, B.F. Fitzgerald, E.A. Gust, D.C. Lawry, J.P. Lazar, and R.L. Oye, "Dynamic thermal rating system relieves transmission constraint," *IEEE 11th Int. Conf. on Transmission & Distribution Construction, Operation and Live-Line Maintenance*, Oct. 2006.

[8] *Overhead Electrical Conductors – Calculation Methods for Stranded Bare Conductors*, IEC Std. TR 1597, 1995

[9] CIGRE Working Group 22.12, "The thermal behavior of overhead line conductors," *Electra*, vol. 144, no. 3, pp. 107-125. 1992.

[10] *IEEE Standard for Calculating the Current-Temperature Relationship of Bare Overhead Conductors*, IEEE Std. 738, Jan. 2007.

[11] A. Michiorri, P.C. Taylor, and S.C.E. Jupe, "Overhead line real-time rating estimation algorithm: description and validation," *Proc. of the Institution of Mechanical Engineers, Part A: Journal of Power and Energy*, vol. 224, no. 3, pp. 293-304, May 2010.

[12] W. Luo, M.C. Taylor, and S.R. Parker, "A comparison of spatial interpolation methods to estimate continuous wind speed surfaces using irregularly distributed data from England and Wales," *Int. Journal of Climatology*, vol. 28, issue 7, pp. 947-959, Jun. 2008.

[13] D.C. Hill, D. McMillan, K.R.W. Bell, and D. Infield, "Application of auto-regressive models to U.K. wind speed data for power system impact studies," *IEEE Trans. on Sustainable Energy*, vol. 3, issue 1, pp. 134-141, Jan. 2012.

[14] Scottish Power Energy Networks, "Implementation of real-time thermal rating," LCNF SPT1001.

[15] G.P. Nason, "Stationary and non-stationary time series," Chapter 11 of *Statistics in Volcanology*, (H.M. Mader, S.G. Coles, C.B. Connor, and L.J. Connor, eds.), Bath: Geological Society, 2006.

[16] Z. Yang, "Fourier analysis-based air temperature movement analysis and forecast," *IET Signal Processing*, vol. 7, issue 1, pp. 14-24, Feb. 2013.

[17] G. Bohling, "Kriging," *Data Analysis in Engineering and Natural Science*, Oct. 2005 [Online]. Available: http://people.ku.edu/~gbohling/cpe940/Kriging.pdf

[18] G. Bohling, "Introduction to geostatistics and variogram analysis," *Data Analysis in Engineering and Natural Science*, Oct. 2005 [Online]. Available: http://people.ku.edu/~gbohling/cpe940/Variograms.pdf

[19] S.R. Vieira, J.R.P. Carvalho, M.B. Ceddia, and A.P. Gonzalez, "De-trending non stationary data for geostatistical applications," *Embrapa Agriculture Informatics*, vol. 69, pp. 1-8, 2010 [Online]. Available: http://www.scielo.br/pdf/brag/v69s0/02.pdf

[20] A. Stepek and I.L. Wijnant, "Interpolating wind speed normal from the sparse Dutch network to a high resolution grid using local roughness from land use maps," Koninklijk Netherlands Meteorological Institute, Tech. Rep. TR-321, Jun. 2011 [Online]. Available: http://www.knmi.nl/bibliotheek/knmipubTR/TR321.pdf

[21] N. Nawri, H. Bjornsson, G.N. Petersen, and K. Jonasson, "Empirical terrain models for surface wind and air temperature over Iceland," Icelandic Meteorological Office, Report no. VI 2012-009, Sep. 2012 [Online]. Available: http://www.vedur.is/media/2012_009_web.pdf

[22] H. Xue, R. Zhu, and Z. Yang, "Study on land wind speed variation in coastal area," *Atca Energiae Solaris Sinica*, vol. 23, no. 2, pp. 207-210, Apr. 2002.

[23] G.E.P. Box, G.M. Jenkins, and G.C. Reinsel, *Time Series Analysis: Forecasting and Control*, 4th Ed., Oxford: Wiley, 2008.

[24] H. Lütkepohl, *New Introduction to Multiple Time Series Analysis*, New York: Springer-Verlag, 2005.

[25] MATLAB Release 2012a, the MathWorks, Inc., Natick, Massachusetts, United States.

[26] C.J. Willmott, K. Matsuura, and S.M. Robeson, "Ambiguities inherent in sums-of-squares-based error statistics," *Atmospheric Environment*, vol. 43, issue 3, pp. 749-752, 2009.

[27] J. Parkes and A. Tindal, "Forecasting short term wind farm production in complex terrain," *in Proc. EWEC Conf.*, London, U.K., 2004.

[28] H. Chai, W. Cheng, C. Zhou, X. Chen, X. Ma, and S. Zhao, "Analysis and comparison of spatial interpolation methods for temperature data in Xinjiang Uygur Autonomous Region, China," *Natural Science*, vol. 3, no. 12, pp. 999-1010, Dec. 2011.